IKKβ signaling mediates metabolic changes in the hypothalamus of a Huntington's disease mouse model

Rana Soylu-Kucharz[1]*, Ali Khoshnan[2] and Åsa Petersén[1]

1. Translational Neuroendocrine Research Unit, Department of Experimental Medical Science, Lund University, BMC D11, SE-22184 Lund, Sweden

2. California Institute of Technology, Pasadena, CA 91125

*Address for correspondence: Rana Soylu-Kucharz

Translational Neuroendocrine Research Unit, BMC D11, 221 84 Lund, Sweden

Email: rana.soylu_kucharz@med.lu.se

Phone: +46 46 222 44 82

Fax: +46 46 222 05 31

Abstract

Background: Huntington's disease (HD) is a neurodegenerative disorder caused by a CAG repeat expansion in the huntingtin (*HTT*) gene. Metabolic changes are associated with HD progression, and underlying mechanisms are not fully known. As the IKKβ/NF-κB pathway is an essential regulator of metabolism, we investigated the involvement of IKKβ, the upstream activator of NF-κB in hypothalamus-specific HD metabolic changes.

Methods: Using viral vectors, we expressed amyloidogenic N-terminal fragments of mutant HTT (mHTT) fragments in the hypothalamus of mice without IKKβ in the CNS ($IKK\beta^{-/-}$) and control mice ($IKK\beta^{+/+}$). We assessed effects on body weight, metabolic hormones, and hypothalamic neuropathology.

Results: Hypothalamic expression of mHTT led to an obese phenotype only in female mice. CNS-specific inactivation of IKKβ prohibited weight gain in females, which was independent of neuroprotection and microglial activation.

Conclusions: The expression of mHTT in the hypothalamus causes metabolic imbalance in a sex-specific fashion, and central inhibition of the IKKβ pathway attenuates the obese phenotype.

Keywords: Huntington's disease, IKKβ pathway, metabolism, hypothalamus, obesity

Introduction

Huntington's disease (HD) is a fatal neurodegenerative disorder caused by a CAG repeat expansion in the huntingtin (HTT) gene (HDCRG, 1993). Although the clinical diagnosis is based on typical motor symptoms, affected individuals also suffer from non-motor symptoms such as cognitive decline, psychiatric symptoms, and metabolic disturbances, which often precede motor symptoms by several years (Bates et al., 2015; Cheong, Gabery, & Petersen, 2019). Metabolic changes in HD include weight loss despite adequate or even higher caloric intake (Aziz et al., 2008; Marder et al., 2009). A higher baseline body mass index (BMI) has been associated with a slower disease progression (van der Burg et al., 2017). Hence, identifying the underlying mechanisms of metabolic changes in HD may reveal novel targets for therapeutic interventions to modify disease progression.

The hypothalamus is a master regulator of metabolism (Cakir & Nillni, 2019; Timper & Bruning, 2017). Imaging studies have identified hypothalamic changes in both prodromal and symptomatic HD patients (Douaud et al., 2006; Kassubek, Gaus, & Landwehrmeyer, 2004; Politis et al., 2008; Soneson et al., 2010). Analyses of postmortem hypothalamic tissue from HD cases and animal models (Cheong et al., 2019) showed loss of neuronal populations expressing orexin (hypocretin), oxytocin, and vasopressin, as well as altered metabolic pathways in several nuclei (Baldo et al., 2019; Gabery, Halliday, Kirik, Englund, & Petersen, 2015; Gabery et al., 2010; Petersen et al., 2005). Inactivation of mutant HTT (mHTT) selectively in the hypothalamus in the transgenic BACHD mouse model prevented developing a metabolic phenotype with obesity accompanied by leptin and insulin resistance (Gray et al., 2008; Hult et al., 2011). Similarly, local expression of mHTT in the hypothalamus using recombinant adeno-associated viral (rAAV) vectors in mice led to hyperphagic obesity with leptin and insulin resistance (Hult et al., 2011;

Soylu-Kucharz, Adlesic, Baldo, Kirik, & Petersen, 2015). Transgene expression was present in several appetite-regulating hypothalamic cell populations (i.e., AGRP, POMC)(Hult et al., 2011). As a result, even though these experiments have proved a causal link between hypothalamic expression of mHTT and the development of metabolic imbalance in mice, the mechanisms of hypothalamic mHTT induced metabolic imbalance are still unknown.

The inhibitor of κB kinase β/ nuclear factor-κB (IKKβ/NF-κB) signaling pathway plays a significant role in obesity and overeating and is enriched in the hypothalamus (Meng & Cai, 2011; X. Zhang et al., 2008). Hyperphagia has been shown to activate IKKβ/NF-κB in the hypothalamus through increased endoplasmic reticulum stress, and suppression of IKKβ/NF-κB results in reduced food intake and normalized metabolic phenotype in mice (Douglass, Dorfman, Fasnacht, Shaffer, & Thaler, 2017; X. Zhang et al., 2008; Y. Zhang, Reichel, Han, Zuniga-Hertz, & Cai, 2017). The IKKβ/NF-kB pathway is also activated by mHTT and has been associated with HD pathogenesis (Atwal et al., 2011; Becanovic et al., 2015; Khoshnan et al., 2004; Sarkar et al., 2011; Thompson et al., 2009; Trager et al., 2014). In the R6/1 mouse model of HD, brain-specific deletion of IKKβ impaired the behavioral phenotype and led to exacerbated neurodegeneration with an activated microglial response in the striatum (Ochaba et al., 2019). However, it is not known whether the IKKβ/NF-κB pathway is involved in the development of HD metabolic imbalance. In the present study, our aim was to determine whether inactivation of the IKKβ/NF-κB pathway would prevent hypothalamic-induced metabolic changes induced by mHTT. We therefore performed injections of rAAV vectors expressing mHTT into the hypothalamus of mice without IKKβ in the CNS ($IKK\beta^{-/-}$) and compared metabolic effects to control mice with the floxed allele of IKKβ ($IKK\beta^{+/+}$).

Materials and methods

Animals

The experimental procedures performed on mice were carried out using the approved guidelines in the ethical permit approved by the Lund University Animal Welfare and Ethics committee in the Lund-Malmö region (ethical permit numbers M20-11 and M65-13). Generation of $IKK\beta^{lox/lox}$ (referred to as $IKK\beta^{+/+}$) mice (Li, Omori, Labuda, Karin, & Rickert, 2003) and Nestin-Cre mice (Betz, Vosshenrich, Rajewsky, & Muller, 1996) was described previously. Nestin/$IKK\beta^{lox/lox}$ (referred to as $IKK\beta^{-/-}$) mice were generated following several generations of backcrossing. Mice were obtained through crossing $IKK\beta^{-/-}$ mice with $IKK\beta^{+/+}$ mice. The experiments were carried out on 2-6 months old mice old, both male and female mice, with the genotypes of $IKK\beta^{-/-}$ mice and their $IKK\beta^{+/+}$ WT littermates. Genotyping for $IKK\beta^{+/+}$ was performed using the following primer sequence 5'-GTC ATT TCC ACA GCC CTG TGA-3' and 5'-CCT TGT CCT ATA GAA GCA CAA C-3', as described previously (Chen et al., 2003). The animals were kept at 12 hours night/day cycle with free access to a standard chow diet and water.

Adeno-associated viral vectors

To investigate the effect of the IKK pathway on the development of the metabolic phenotype, we performed stereotactic injections of recombinant adeno-associated viral (rAAV) vectors into the hypothalamus of $IKK\beta^{+/+}$ and $IKK\beta^{-/-}$ mice. The viral vector was a pseudotyped rAAV2/5 vector (transgene was flanked by two inverted terminal repeats of the AAV2 and packaged in an AAV5 capsid), where the human mHTT gene of 853 amino acids length (853HTT79Q) (Hult et al., 2011). The human Synapsin-1 promoter drove the mHTT gene expression.

104

105 **Viral vector injections**

106 The animals were anesthetized by air mask inhalation of isoflurane (2% isoflurane in O2/N2O
107 (3:7)). The mouse head was fixed with a nose clamp and ear bars in the stereotaxic apparatus.
108 Following the head position's fine-tuning on the stereotaxic frame, the skull was thinned with a
109 dental drill to make a borehole at the determined anterior-posterior and medial-lateral
110 hypothalamic coordinates. Subsequently, the final dorsal-ventral coordinates were measured from
111 the dura mater. The stereotaxic coordinates chosen for hypothalamic injections were: 0.6 mm
112 posterior to bregma, -0.6 mm lateral to the bregma, and 5.2 mm ventral to the dura mater, selected
113 according to the mouse brain atlas (Franklin & Paxinos, 2008).

114 The rAAV vector delivery was performed bilaterally in the hypothalamus. The silica glass
115 capillary (with an outer diameter of ~ 80 µm) attached to a 5 µl Hamilton syringe (Nevada, USA)
116 was used for the virus delivery. A total volume of 0.5 µl viral vector solution was pulled in a glass
117 capillary, and the capillary was descended from dura mater to target coordinates slowly. At the
118 target, the first 0.1 µl of the total volume was injected. After 30 seconds, the viral suspension was
119 delivered at a rate of 0.05µl/15s until the whole volume was delivered. To allow the brain to absorb
120 the viral vector solution, the capillary was left at the target for an additional 5 minutes at the end
121 of the injection. The viral vector concentration used in the study was 2,1E+14 genome copies
122 (GC)/ml.

123

124 **Perfusion and serum collection**

To induce deep anesthesia in mice, a terminal dose of pentobarbital (600 mg/kg, Apoteksbolaget) was injected intraperitoneally. The thoracic cavity was opened to expose the heart, and blood was collected from the right ventricle with the 16G needle. Subsequently, a small incision was made to insert a 12-gauge perfusion needle at the tip of the left ventricle. First, the vessels were rinsed with the saline solution at a rate of 10-12 ml/min for a minute, and then it was switched to freshly prepared 4% paraformaldehyde (PFA) ~0°C for 8 minutes. Following that, the animals were decapitated, and the brains were isolated. The brains were placed in 4% PFA for 24 hours at 4°C for post-fixation. Next, the PFA was replaced with 25% sucrose solution at 4°C for cryoprotection (~24 hours).

Finally, the fixed brains were sectioned coronally on a semi-automated freezing microtome (Microm HM 450) at 30 µm thick slices and in six series. Until further processing, the brain sections were stored in antifreeze solution (30% glycerol and 30% ethylene glycol in phosphate buffer) at −20 °C.

Metabolic Measurements

Serum insulin and leptin concentrations were assessed in blood collected from the heart left ventricle prior to perfusion. The blood was kept at room temperature for 30 minutes to clot and spun for 15 minutes at 2500 g. The serum (supernatant) was stored at -80 C. Serum levels of insulin (Crystal Chem Inc, Catalog #90080) and leptin (Crystal Chem Inc, Catalog #90030) were assessed using ELISA according to the manufacturer's instructions.

146 **Immunohistochemistry**

147 The free-floating brain sections were used for immunohistochemistry (IHC). All the washing steps
148 (10 minutes/wash) and incubations were performed using gentle agitation on a shaker at room
149 temperature. The sections were washed three times in Tris-buffered-saline (TBS) in 1% Triton X
150 (TBS-T) to remove the antifreeze solution. The endogenous peroxidase activity was blocked by
151 30 minutes of incubation in 10% methanol with 3% H_2O_2 in TBS. Following that, the sections
152 were washed three times for 10 minutes in TBS-T. The sections were incubated with 5% serum
153 and bovine serum albumin (BSA) in TBS-T for 1 hour to reduce nonspecific binding of the primary
154 and secondary antibodies. Next, the sections were left in the respective primary antibody solutions
155 in 3% appropriate corresponding serum in TBS-T (anti-huntingtin (sc-8767; 1:500; goat; Santa
156 Cruz), anti-ubiquitin (1:2000; rabbit; Dako), anti-orexin (1:4000; rabbit; Phoenix
157 Pharmaceuticals), anti-tyrosine hydroxylase (1:2000; rabbit; Pel-Freez), anti-GnRH (1:3000, anti-
158 rabbit, Abcam #ab5617), anti-iba-1) and left on shaker for overnight incubation at room
159 temperature. Next, sections were washedthree3 times for 10 minutes in TBS-T. The secondary
160 antibody incubation was performed in 3% respective serum or BSA with TBS-T for 1 hour at room
161 temperature, and the sections were washed three times for 10 minutes in TBS before 3,3′-
162 diaminobenzidine (DAB) development (Vectastain, ABC kit). Brain sections were mounted on
163 chromatin-gelatin coated glass slides. The air-dried sections were left in distilled water for 1
164 minute and dehydrated in increasing ethanol solutions (70%, 95%, 99%). Finally, the samples were
165 cleared in xylene and covered with glass coverslips using DPX mounting medium (Sigma-
166 Aldrich).

167

Stereological analyses

To estimate the numbers of cells positive for orexin, TH, GnRH (in the anterior hypothalamus; AHA), and size of the inclusions, we applied unbiased stereological quantification principles by using the optical dissector method (West, Slomianka, & Gundersen, 1991). Stereological analyses were performed with a Nikon 80i microscope, which is equipped with an X–Y motorized stage (Märzhauser, Wetzlar) and a high precision linear encoder (Heidenhain, Traunreut). The position of the stage and the input from the digital camera were controlled by a computer. The sampling interval was adjusted to count at least 100 cells for each hypothalamus to minimize the coefficient of error. The region of interest was delineated under the 4X objective, whereas the counting was performed using a 60X NA 1.4 Plan-Apo oil objective with a random start systematic sampling routine (NewCast Module in VIS software; Visiopharm A/S, Horsholm). The border delineation processes for orexin, TH, GnRH cell populations were defined by the natural contours of cell populations. The number and size of iba-1 positive microglia/macrophages were quantified in the anatomical borders of the mediobasal hypothalamus. The number of small, medium and large size HTT inclusions was quantified with HTT staining (sc-6787). The inclusions ~ 0.04 - 0.1 µm size considered small, 0.15 - 0.25 µm medium and ~ 0.25-0.5 µm large size inclusions. The same size of the area was quantified for all genotypes and gender under blinded conditions. The mean number of assessed inclusions per brain was 755, median 663 with a standard deviation of error 528 inclusions.

Metabolic tests

For all animals used in the study, body weight was measured bimonthly. Serum insulin and leptin concentrations were assessed in serum. Blood was collected from the heart left ventricle at 18 weeks post-injection, and they were kept at room temperature for 30 minutes to clot, spun for 15 minutes at 2500 g. Serum (supernatant) was aliquoted and stored at -80 C. Serum levels of leptin (Crystal Chem Inc, Catalog #90030) and testosterone (Demeditec, Cat.-No.: DEV9911) were determined with ELISA according to the manufacturer's instructions.

Statistical analysis

All statistical analyses were performed using Prism 8 software (GraphPad). The data was initially tested with D'Agostino & Pearson omnibus normality test for normal distribution. Following that, the data was either subjected to Kruskal–Wallis followed by Dunn's multiple comparison tests or an unpaired t-test with equal SD. The statistical test results and the type of analysis used for each experiment are specified in detail in the results section and figure legends. Statistically significant differences were considered for $p<0.05$.

Results

Inhibition of the IKKβ pathway protects from hypothalamic mHTT-induced obesity in female mice

To assess the effects of mHTT expression on the development of a metabolic phenotype, we injected IKK$\beta^{+/+}$ (homozygous for the floxed allele of IKKβ, control group) and IKK$\beta^{-/-}$

(expressing Cre-recombinase under nestin promotor) mice with rAAV vectors expressing mHTT (AAV5-853HTT79Q vectors are referred to as HD elsewhere) in the hypothalamus of both sexes. Consistent with our previous findings (Baldo, Soylu, & Petersen, 2013; Hult et al., 2011; Soylu-Kucharz et al., 2015), expression of mHTT in female control mice led to an obese phenotype (**Figure 1A, C).** The body weight at 18 weeks post-injection was significantly higher in the IKKβ$^{+/+}$HD mice (n=16 and mean= 55.6g, SD=10.2) compared to IKKβ$^{-/-}$HD mice (n=20 and mean=40.6g, SD=9.3, $p<0.0001$) and uninjected mice of the two genotypes (uninjected IKKβ$^{+/+}$: n=15 and mean=43.7g, SD=7.4, $p=0.0026$; uninjected IKKβ$^{-/-}$: n=13 and mean=37.1g, SD=9.8, $p<0.0001$). Hence, inactivation of the IKKβ pathway in Nestin-expressing cells protected female mice from hypothalamic mHTT induced obesity **(Figure 1A)**. The brain-specific deletion of IKKβ did not affect the circulating insulin and leptin levels in mice (Meng & Cai, 2011). Therefore, in this study, we assessed the serum levels of insulin and leptin levels only in mice expressing mHTT in the hypothalamus. In line with the prevention of body weight gain, IKKβ$^{-/-}$HD mice displayed significantly lower serum levels of insulin and leptin than IKKβ$^{+/+}$HD mice **(Figure 1D)**.

IKKβ did not affect the body weight in male mice with or without injections of AAV5-853HTT79Q as assessed up to 18 weeks post-injection **(Figure 1B, F)**. However, analyses of serum levels of insulin and leptin showed that even though there was no effect on body weight, levels of insulin and leptin were significantly elevated in IKKβ$^{-/-}$HD mice compared to IKKβ$^{+/+}$HD mice **(Figure 1G and 1H)**.

IKKβ is not involved in the mHTT-mediated loss of orexin and TH positive cell populations in HD mice

The development of the metabolic phenotype in HD has been associated with expression of mHTT in the hypothalamus (Hult et al., 2011; Soylu-Kucharz et al., 2015). Here we tested whether the rescue of the metabolic phenotype observed in IKKβ$^{-/-}$HD mice was due to the preservation of metabolism-regulating neuronal populations known to be affected in HD (Cheong et al., 2019). In female mice, there was no benefit of IKKβ silencing as the number of orexin positive cells was comparable in IKKβ$^{+/+}$HD (cell loss ~64%) and IKKβ$^{-/-}$HD groups (cell loss ~82%), and both groups had a significantly lower number of orexin cells compared to uninjected groups of female mice **(Figure 2A and 2B)**. Male IKKβ$^{-/-}$HD mice had significantly lower orexin and A13 TH positive cells than IKKβ$^{+/+}$HD mice in the hypothalamus **(Supplementary Figure 1A and 1B)**.

The loss of A13 TH positive cells was ~80% in IKKβ$^{-/-}$HD and ~65% in IKKβ$^{+/+}$HD when compared to WT and IKKβ$^{-/-}$ uninjected female mice **(Figure 2C and 2D)**.

Reduced testosterone levels are associated with increased circulating levels of leptin and insulin, even in the absence of increased BMI (Luukkaa et al., 1998; Pitteloud et al., 2005). The hypothalamic-pituitary-gonadal (HPG) axis, which regulates testosterone production, is altered in HD (Bird, Chiappa, & Fink, 1976; Kalliolia et al., 2015; Markianos, Panas, Kalfakis, & Vassilopoulos, 2005; Papalexi et al., 2005; Petersen & Bjorkqvist, 2006; Saleh et al., 2009; Soylu-Kucharz, Baldo, & Petersen, 2016; Van Raamsdonk et al., 2007). The number of GnRH positive cells was comparable **(Figure 2F and Supplementary Figure 1C)**; however, the total circulating level of testosterone was diminished in IKKβ$^{-/-}$HD male mice by 60% compared to IKKβ$^{+/+}$HD male mice expressing mHTT in the hypothalamus **(Supplementary Figure 1D)**.

The number or size of Iba-1 positive microglial cells in the mediobasal hypothalamus.

Given that IKKβ is one of the mediators of microglial activation and energy balance (Karin, 1999; Liu, Zhang, Joo, & Sun, 2017), we investigated whether protection from hypothalamic mHTT induced obesity in IKKβ$^{-/-}$ female mice was due to alteration in microglial activation. Nonetheless, the number and size of Iba1 positive cells in the mediobasal hypothalamus of both IKKβ$^{+/+}$HD and IKKβ$^{-/-}$HD female mice were comparable **(Figure 3A-C)**.

IKKβ$^{-/-}$HD female mice display an increased number of small-sized inclusions of mHTT

Reduction of IKKβ activity decreases the cleavage of both WT and mHTT and prevents the accumulation of mHTT inclusions (Khoshnan, Ko, Tescu, Brundin, & Patterson, 2009; Thompson et al., 2009). IKKβ silencing studies also showed impaired clearance of mHTT and worsening HD pathological phenotypes in vivo and vitro (Khoshnan et al., 2009; Thompson et al., 2009). In our model, inclusions were increased in IKKβ$^{-/-}$HD compared to IKKβ$^{+/+}$HD in both female and male mice **(Figure 4A-C)**. The small size inclusions were responsible for the increase, as the number of medium or large size inclusions were similar between IKKβ$^{+/+}$HD and IKKβ$^{-/-}$HD groups **(Figure 4D-F)**. Altogether, these results show the increase in inclusion formation correlates with previous reports on IKKβ silencing in HD (Criollo et al., 2010; Khoshnan et al., 2009; Ochaba et al., 2019).

Discussion

Alterations in energy metabolism may affect disease progression in HD as weight loss is part of the clinical phenotype, and a higher BMI has been associated with the slower clinical decline (van der Burg et al., 2017). Understanding the underlying biological cause of metabolic disturbances in

HD may unravel novel therapeutic targets for this fatal neurodegenerative disorder. The IKKβ/NF-κB pathway has been implicated in HD pathogenesis (Khoshnan & Patterson, 2011), but it has not been investigated in the context of HD metabolic and hypothalamic alterations. Here, we expressed mHTT in the hypothalamus of control mice and compared effects to mice with IKKβ inactivated in the CNS. We found that hypothalamic mHTT expression induces obese phenotype selectively in the female mice and inactivation of the IKKβ prevents it. Gender differences play a role in HD as the severity and rate of the motor symptoms progression has been suggested to be faster in women than men with HD (Zielonka et al., 2013; Zielonka et al., 2018; Zielonka & Stawinska-Witoszynska, 2020). Previous studies indicated that sex also affects the HD metabolic and behavioral manifestation in animal models (Dorner, Miller, Barton, Brock, & Rebec, 2007; Sjogren et al., 2019; Soylu-Kucharz et al., 2016). Even though the expression of mHTT in the hypothalamus of male mice did not affect body weight, male IKKβ$^{-/-}$HD displayed high serum leptin and insulin levels. As testosterone deficiency is associated with metabolic syndrome exemplified by increased circulating leptin levels and insulin resistance, it is possible that the increase in serum leptin and insulin levels could be due to reduced circulating testosterone levels in IKKβ$^{-/-}$HD mice.

Obese phenotype can occur due to increased caloric intake, decreased activity, metabolic rate, or combination of these factors. Previously, we demonstrated that the obese phenotype caused by hypothalamic mHTT expression was due to hyperphagia as general motor activity and basal metabolic rate were unaltered in these mice (Hult et al., 2011). The mice in this study were housed in a separate animal unit that lacks behavior testing platforms and limiting the number of in-house cages. Therefore, we were not able to re-test basic parameters such as food intake and locomotor activity. However, as we have previously shown that obese phenotype was caused by increased

297 food intake, we speculate that the silencing of the IKKβ expression prohibited hyperphagia-
298 induced obesity in HD mice. The orexin and A13 TH neuronal populations are involved in
299 metabolism regulation (Adeghate et al., 2020; Shi et al., 2013) and they are affected in HD (Gabery
300 et al., 2010; Hult et al., 2011; Petersen et al., 2005; Soylu-Kucharz et al., 2015). As the inactivation
301 of the IKKβ signaling did not affect the preservation of these cells, we can speculate that orexin
302 and A13 TH neuropathology are not the central cell populations responsible for the development
303 of HD bodyweight alterations.

304 In conclusion, our study shows that hypothalamic expression of mHTT leads to a metabolic
305 imbalance in a sex-specific fashion. The weight gain phenotype induced by the mHTT in female
306 mice is prevented by IKKβ inactivation and is independent of orexin TH neuroprotection, and
307 microglial activation.

308

309 **Author contributions statements**

310 RS, ÅP, and AK conceived and designed the experiments. RSK performed the experiments. RSK
311 and ÅP analyzed the data. RSK and ÅP wrote the first draft of the manuscript. All authors were
312 involved in editing the manuscript and approved the final version.

313

314 **Conflict of interest**

315 The authors declare no conflict of interest.

316

317 **Figure legends**

Figure 1: Inactivation of the IKKβ pathway inhibits the development of obesity-induced by mHTT expression in the hypothalamus of female mice

IKKβ$^{+/+}$ and IKKβ$^{-/-}$ mice were injected bilaterally into the hypothalamus with AAV-HTT853-79Q vectors and assessed using metabolic analyses. **(A)** Female IKKβ$^{+/+}$ mice develop increased body weight after hypothalamic injections of AAV5-HTT853-79Q vectors which is prevented in IKKβ$^{-/-}$ female mice (two-way repeated measures ANOVA, effect of time $F(2, 62) = 8.920$, $p<0.0001$; effect of genotype $F(1, 31) = 20.83$, $p<0.0001$; effect of genotype x time $F(2, 62) = 8.920$, $p=0.0004$; followed by a Sidak's multiple comparisons test: $p= 0.0026$ at 8 weeks and $p< 0.0001$ at 18 weeks). **(B)** Male IKKβ$^{+/+}$ and IKKβ$^{-/-}$ mice do not develop obesity after AAV5-HTT853-79Q vector injections (two-way repeated measures ANOVA, effect of time $F(2, 72) = 190.4$, $P < 0.0001$; effect of genotype $F(1, 36) = 2.359$, $P = 0.1333$; effect of genotype x time $F(2, 72) = 1.446$, $P = 0.2422$, followed by a Sidak's multiple comparisons test). **(C)** Body weight changes at 18 weeks post-injection in females (One-way ANOVA, effect of treatment $F(3, 60) = 11.69$, $P<0.0001$ followed by Sidak's multiple comparisons test). Serum **(D)** insulin (two-tailed, unpaired t-test, n=16/19, p=0.0082) and **(E)** leptin (two-tailed, Mann Whitney test, n=16/19, p=0.0003) concentrations measured by ELISA in females at 18 weeks post injection. **(F)** Body weight changes at 18 weeks post-injection in males (One-way ANOVA, effect of treatment $F(3, 55) = 0.7312"$, $P=0.5378$ followed by Sidak's multiple comparisons test). Serum **(G)** insulin (two-tailed, Mann Whitney test, n=15/21, p=0.0448) and **(H)** leptin (two-tailed, unpaired t-test, n=15/21, p=0.0023) assessments at 18 weeks. Data are represented as box and whisker plots (25–75 percentile (boxes), min to max (whiskers), median (horizontal line), mean (+)).

Figure 2: Quantitative analysis of the neuronal populations expressing orexin, TH in the A13 area, and GnRH in female mice at 18-week post-injection of AAV-HTT853-79Q vectors. (A) Representative immunohistochemically stained sections show orexin immunopositive cells in the hypothalamus. **(B)** Stereological analysis of orexin immunopositive cells in female mice at the 18 weeks time point (Kruskal-Wallis test followed by Dunn's multiple comparisons test p=0.0002; n=4-8/group). **(C)** Representative photomicrographs show the A13 TH immunopositive cell population in the hypothalamus. **(D)** Numbers of A13 TH positive cells in the hypothalamus's zona incerta area (Kruskal-Wallis test followed by Dunn's multiple comparisons test p=0.0001; n=4-9/group). **(E)** Representative photomicrographs illustrate the GnRH positive cells in the anterior hypothalamic area of the hypothalamus. **(F)** Stereological quantification of GnRH positive cells in the anterior hypothalamic area (Kruskal-Wallis test followed by Dunn's multiple comparisons p=0.0802; n=4-8/group). Points on scatter graphs represent total cell count for individual mice, the lines are means, and the whiskers indicate ± SEM. Scale bars represent 200 μm.

Figure 3: No effect of the IKKβ pathway on the degree of iba-1 positive cell activation at 18 weeks post-injection in females. Stereological assessment of **(A)** the total number of iba-1 positive cells (two-tailed, unpaired t-test, n=7/8, p=0.477) and **(B)** the size of Iba-1 positive cells (two-tailed, Mann-Whitney test, n=7/8 animals, n=783/911 cells/genotype, p=0.9601) in the mediobasal hypothalamus (MBH) 18 weeks after injections of AAV5-HTT853-79Q vectors in IKKβ$^{+/+}$ and IKKβ$^{-/-}$ mice. In (A), data are represented as scatter dot plots, and bars represent mean ± SEM, and in (B), data are represented as scatter dot plots, and lines represent median.

Figure 4: Inactivation of the IKKβ pathway leads to increased numbers of huntingtin inclusions in the hypothalamus. Representative photomicrographs of sections processed for immunohistochemistry for **(A)** huntingtin (using the sc-8767 antibody) and **(B)** ubiquitin demonstrating the formation of inclusions in the hypothalamus after injections of AAV-HTT853-79Q vectors in IKKβ$^{+/+}$ and IKKβ$^{-/-}$ mice. Stereological quantification of sections processed with the huntingtin antibody show **(C)** the total number of inclusions (Females: two-tailed, Mann-Whitney test, n=5/group, p=0.0008; Males: two-tailed, Mann-Whitney test, n=5/group, p<0.0001), (D) large-sized inclusions (Females: two-tailed, Mann-Whitney test, n=5/group, p=0.3095; Males: two-tailed, unpaired t-test, n=5/group, p=0.8992), **(E)** medium-sized inclusions (Females: two-tailed, unpaired t-test, n=5/group, p=0.0635); Males: two-tailed, unpaired t-test, n=5/group, p=0.0911) and **(F)** small-sized inclusions (Females: two-tailed, Mann-Whitney test, n=5/group, p=0.0079; Males: two-tailed, unpaired t-test, n=5/group, p<0.0001) inclusions in female and male mice at 18 weeks post-injection. Points on scatter graphs represent total inclusion count for individual mice, the lines are means, and the whiskers indicate ± SEM. Scale bars represent 200 μm and 25 μm on lower and higher magnifications, respectively.

Supplementary figure 1: Effects on the orexin, GnRH, and A13 TH cell populations in the hypothalamus in male mice after injections of AAV-HTT853-79Q vectors. Stereological quantification of **(A)** orexin (two-tailed, unpaired t-test, n=8/group, p=0.001), **(B)** TH (two-tailed, unpaired t-test, n=8/group, p=0.0471) and **(C)** GnRH (two-tailed, unpaired t-test, n=7/group, p=0.3648) positive cells in IKKβ$^{+/+}$ and IKKβ$^{-/-}$ males expressing mHTT in the hypothalamus at 18 weeks post-injection. **(D)** Changes in serum testosterone levels in male IKKβ$^{+/+}$ and IKKβ$^{-/-}$ mice at 18 weeks post-injection of AAV-853HTT-79Q in the hypothalamus (two-tailed, Mann-

Whitney test, n=8/14, p=0.0159). Data are represented as scatter dot plots, the lines are means, and the whiskers indicate ± SEM**.**

Acknowledgments

This work was supported by grants from the Swedish Medical Research Council (grant numbers 2013/03537 and 2018/02559), the Province of Skåne State Grants (ALF) as well as the Knut and Alice Wallenberg Foundation (# 2019.0467) to ÅP. ÅP is a Wallenberg Clinical Scholar (Knut and Alice Wallenberg Foundation # 2019.0467). RSK was supported by Svenska Sällskapet för Medicinsk Forskning fellowship. We are grateful for the excellent technical assistance provided by Björn Anzelius, Anneli Josefsson, Ulla Samuelsson and Ulrika Sparrhult-Bjork at Lund University.

References:

Adeghate, E., Lotfy, M., D'Souza, C., Alseiari, S. M., Alsaadi, A. A., & Qahtan, S. A. (2020). Hypocretin/orexin modulates body weight and the metabolism of glucose and insulin. *Diabetes Metab Res Rev, 36*(3), e3229. doi:10.1002/dmrr.3229

Atwal, R. S., Desmond, C. R., Caron, N., Maiuri, T., Xia, J., Sipione, S., & Truant, R. (2011). Kinase inhibitors modulate huntingtin cell localization and toxicity. *Nat Chem Biol, 7*(7), 453-460. doi:10.1038/nchembio.582

Aziz, N. A., van der Burg, J. M., Landwehrmeyer, G. B., Brundin, P., Stijnen, T., Group, E. S., & Roos, R. A. (2008). Weight loss in Huntington disease increases with higher CAG repeat number. *Neurology, 71*(19), 1506-1513. doi:10.1212/01.wnl.0000334276.09729.0e

Baldo, B., Gabery, S., Soylu-Kucharz, R., Cheong, R. Y., Henningsen, J. B., Englund, E., . . . Petersen, A. (2019). SIRT1 is increased in affected brain regions and hypothalamic

metabolic pathways are altered in Huntington disease. *Neuropathol Appl Neurobiol, 45*(4), 361-379. doi:10.1111/nan.12514

Baldo, B., Soylu, R., & Petersen, A. (2013). Maintenance of basal levels of autophagy in Huntington's disease mouse models displaying metabolic dysfunction. *PloS one, 8*(12), e83050. doi:10.1371/journal.pone.0083050

Bates, G. P., Dorsey, R., Gusella, J. F., Hayden, M. R., Kay, C., Leavitt, B. R., . . . Tabrizi, S. J. (2015). Huntington disease. *Nat Rev Dis Primers, 1*, 15005. doi:10.1038/nrdp.2015.5

Becanovic, K., Norremolle, A., Neal, S. J., Kay, C., Collins, J. A., Arenillas, D., . . . Leavitt, B. R. (2015). A SNP in the HTT promoter alters NF-kappaB binding and is a bidirectional genetic modifier of Huntington disease. *Nat Neurosci, 18*(6), 807-816. doi:10.1038/nn.4014

Betz, U. A., Vosshenrich, C. A., Rajewsky, K., & Muller, W. (1996). Bypass of lethality with mosaic mice generated by Cre-loxP-mediated recombination. *Curr Biol, 6*(10), 1307-1316. doi:10.1016/s0960-9822(02)70717-3

Bird, E. D., Chiappa, S. A., & Fink, G. (1976). Brain immunoreactive gonadotropin-releasing hormone in Huntington's chorea and in non-choreic subjects. *Nature, 260*(5551), 536-538.

Cakir, I., & Nillni, E. A. (2019). Endoplasmic Reticulum Stress, the Hypothalamus, and Energy Balance. *Trends Endocrinol Metab, 30*(3), 163-176. doi:10.1016/j.tem.2019.01.002

Chen, L. W., Egan, L., Li, Z. W., Greten, F. R., Kagnoff, M. F., & Karin, M. (2003). The two faces of IKK and NF-kappaB inhibition: prevention of systemic inflammation but increased local injury following intestinal ischemia-reperfusion. *Nat Med, 9*(5), 575-581. doi:10.1038/nm849

Cheong, R. Y., Gabery, S., & Petersen, A. (2019). The Role of Hypothalamic Pathology for Non-Motor Features of Huntington's Disease. *Journal of Huntington's disease, 8*(4), 375-391. doi:10.3233/JHD-190372

Criollo, A., Senovilla, L., Authier, H., Maiuri, M. C., Morselli, E., Vitale, I., . . . Kroemer, G. (2010). The IKK complex contributes to the induction of autophagy. *The EMBO journal, 29*(3), 619-631. doi:10.1038/emboj.2009.364

Dorner, J. L., Miller, B. R., Barton, S. J., Brock, T. J., & Rebec, G. V. (2007). Sex differences in behavior and striatal ascorbate release in the 140 CAG knock-in mouse model of Huntington's disease. *Behavioural brain research, 178*(1), 90-97. doi:10.1016/j.bbr.2006.12.004

Douaud, G., Gaura, V., Ribeiro, M. J., Lethimonnier, F., Maroy, R., Verny, C., . . . Remy, P. (2006). Distribution of grey matter atrophy in Huntington's disease patients: a combined

ROI-based and voxel-based morphometric study. *NeuroImage, 32*(4), 1562-1575. doi:10.1016/j.neuroimage.2006.05.057

Douglass, J. D., Dorfman, M. D., Fasnacht, R., Shaffer, L. D., & Thaler, J. P. (2017). Astrocyte IKKbeta/NF-kappaB signaling is required for diet-induced obesity and hypothalamic inflammation. *Molecular metabolism, 6*(4), 366-373. doi:10.1016/j.molmet.2017.01.010

Franklin, K. P., & Paxinos, G. (2008). *The Mouse Brain in Stereotaxic Coordinates* (3rd ed.). New York: Academic Press.

Gabery, S., Halliday, G., Kirik, D., Englund, E., & Petersen, A. (2015). Selective loss of oxytocin and vasopressin in the hypothalamus in early Huntington disease: a case study. *Neuropathol Appl Neurobiol, 41*(6), 843-848. doi:10.1111/nan.12236

Gabery, S., Murphy, K., Schultz, K., Loy, C. T., McCusker, E., Kirik, D., . . . Petersen, A. (2010). Changes in key hypothalamic neuropeptide populations in Huntington disease revealed by neuropathological analyses. *Acta neuropathologica, 120*(6), 777-788. doi:10.1007/s00401-010-0742-6

Gray, M., Shirasaki, D. I., Cepeda, C., Andre, V. M., Wilburn, B., Lu, X. H., . . . Yang, X. W. (2008). Full-length human mutant huntingtin with a stable polyglutamine repeat can elicit progressive and selective neuropathogenesis in BACHD mice. *The Journal of neuroscience : the official journal of the Society for Neuroscience, 28*(24), 6182-6195. doi:10.1523/JNEUROSCI.0857-08.2008

HDCRG. (1993). A novel gene containing a trinucleotide repeat that is expanded and unstable on Huntington's disease chromosomes. The Huntington's Disease Collaborative Research Group. *Cell, 72*(6), 971-983.

Hult, S., Soylu, R., Bjorklund, T., Belgardt, B. F., Mauer, J., Bruning, J. C., . . . Petersen, A. (2011). Mutant huntingtin causes metabolic imbalance by disruption of hypothalamic neurocircuits. *Cell metabolism, 13*(4), 428-439. doi:10.1016/j.cmet.2011.02.013

Kalliolia, E., Silajdzic, E., Nambron, R., Costelloe, S. J., Martin, N. G., Hill, N. R., . . . Warner, T. T. (2015). A 24-Hour Study of the Hypothalamo-Pituitary Axes in Huntington's Disease. *PloS one, 10*(10), e0138848. doi:10.1371/journal.pone.0138848

Karin, M. (1999). How NF-kappaB is activated: the role of the IkappaB kinase (IKK) complex. *Oncogene, 18*(49), 6867-6874. doi:10.1038/sj.onc.1203219

Kassubek, J., Gaus, W., & Landwehrmeyer, G. B. (2004). Evidence for more widespread cerebral pathology in early HD: an MRI-based morphometric analysis. *Neurology, 62*(3), 523-524; author reply 524.

Khoshnan, A., Ko, J., Tescu, S., Brundin, P., & Patterson, P. H. (2009). IKKalpha and IKKbeta regulation of DNA damage-induced cleavage of huntingtin. *PloS one, 4*(6), e5768. doi:10.1371/journal.pone.0005768

Khoshnan, A., Ko, J., Watkin, E. E., Paige, L. A., Reinhart, P. H., & Patterson, P. H. (2004). Activation of the IkappaB kinase complex and nuclear factor-kappaB contributes to mutant huntingtin neurotoxicity. *The Journal of neuroscience : the official journal of the Society for Neuroscience, 24*(37), 7999-8008. doi:10.1523/JNEUROSCI.2675-04.2004

Khoshnan, A., & Patterson, P. H. (2011). The role of IkappaB kinase complex in the neurobiology of Huntington's disease. *Neurobiology of disease, 43*(2), 305-311. doi:10.1016/j.nbd.2011.04.015

Li, Z. W., Omori, S. A., Labuda, T., Karin, M., & Rickert, R. C. (2003). IKK beta is required for peripheral B cell survival and proliferation. *Journal of immunology, 170*(9), 4630-4637. doi:10.4049/jimmunol.170.9.4630

Liu, T., Zhang, L., Joo, D., & Sun, S. C. (2017). NF-kappaB signaling in inflammation. *Signal Transduct Target Ther, 2*. doi:10.1038/sigtrans.2017.23

Luukkaa, V., Pesonen, U., Huhtaniemi, I., Lehtonen, A., Tilvis, R., Tuomilehto, J., . . . Huupponen, R. (1998). Inverse correlation between serum testosterone and leptin in men. *J Clin Endocrinol Metab, 83*(9), 3243-3246. doi:10.1210/jcem.83.9.5134

Marder, K., Zhao, H., Eberly, S., Tanner, C. M., Oakes, D., Shoulson, I., & Huntington Study, G. (2009). Dietary intake in adults at risk for Huntington disease: analysis of PHAROS research participants. *Neurology, 73*(5), 385-392. doi:10.1212/WNL.0b013e3181b04aa2

Markianos, M., Panas, M., Kalfakis, N., & Vassilopoulos, D. (2005). Plasma testosterone in male patients with Huntington's disease: relations to severity of illness and dementia. *Annals of neurology, 57*(4), 520-525. doi:10.1002/ana.20428

Meng, Q., & Cai, D. (2011). Defective hypothalamic autophagy directs the central pathogenesis of obesity via the IkappaB kinase beta (IKKbeta)/NF-kappaB pathway. *The Journal of biological chemistry, 286*(37), 32324-32332. doi:10.1074/jbc.M111.254417

Ochaba, J., Fote, G., Kachemov, M., Thein, S., Yeung, S. Y., Lau, A. L., . . . Steffan, J. S. (2019). IKKbeta slows Huntington's disease progression in R6/1 mice. *Proceedings of the National Academy of Sciences of the United States of America, 116*(22), 10952-10961. doi:10.1073/pnas.1814246116

Papalexi, E., Persson, A., Bjorkqvist, M., Petersen, A., Woodman, B., Bates, G. P., . . . Popovic, N. (2005). Reduction of GnRH and infertility in the R6/2 mouse model of Huntington's disease. *The European journal of neuroscience, 22*(6), 1541-1546. doi:10.1111/j.1460-9568.2005.04324.x

Petersen, A., & Bjorkqvist, M. (2006). Hypothalamic-endocrine aspects in Huntington's disease. *The European journal of neuroscience, 24*(4), 961-967. doi:10.1111/j.1460-9568.2006.04985.x

Petersen, A., Gil, J., Maat-Schieman, M. L., Bjorkqvist, M., Tanila, H., Araujo, I. M., . . . Brundin, P. (2005). Orexin loss in Huntington's disease. *Human molecular genetics, 14*(1), 39-47. doi:10.1093/hmg/ddi004

Pitteloud, N., Hardin, M., Dwyer, A. A., Valassi, E., Yialamas, M., Elahi, D., & Hayes, F. J. (2005). Increasing insulin resistance is associated with a decrease in Leydig cell testosterone secretion in men. *J Clin Endocrinol Metab, 90*(5), 2636-2641. doi:10.1210/jc.2004-2190

Politis, M., Pavese, N., Tai, Y. F., Tabrizi, S. J., Barker, R. A., & Piccini, P. (2008). Hypothalamic involvement in Huntington's disease: an in vivo PET study. *Brain : a journal of neurology, 131*(Pt 11), 2860-2869. doi:10.1093/brain/awn244

Saleh, N., Moutereau, S., Durr, A., Krystkowiak, P., Azulay, J. P., Tranchant, C., . . . Maison, P. (2009). Neuroendocrine disturbances in Huntington's disease. *PloS one, 4*(3), e4962. doi:10.1371/journal.pone.0004962 [doi]

Sarkar, S., Korolchuk, V. I., Renna, M., Imarisio, S., Fleming, A., Williams, A., . . . Rubinsztein, D. C. (2011). Complex inhibitory effects of nitric oxide on autophagy. *Molecular cell, 43*(1), 19-32. doi:10.1016/j.molcel.2011.04.029

Shi, Y. C., Lau, J., Lin, Z., Zhang, H., Zhai, L., Sperk, G., . . . Lin, S. (2013). Arcuate NPY controls sympathetic output and BAT function via a relay of tyrosine hydroxylase neurons in the PVN. *Cell metabolism, 17*(2), 236-248. doi:10.1016/j.cmet.2013.01.006

Sjogren, M., Soylu-Kucharz, R., Dandunna, U., Stan, T. L., Cavalera, M., Sandelius, A., . . . Bjorkqvist, M. (2019). Leptin deficiency reverses high metabolic state and weight loss without affecting central pathology in the R6/2 mouse model of Huntington's disease. *Neurobiology of disease, 132*, 104560. doi:10.1016/j.nbd.2019.104560

Soneson, C., Fontes, M., Zhou, Y., Denisov, V., Paulsen, J. S., Kirik, D., . . . Huntington Study Group, P.-H. D. i. (2010). Early changes in the hypothalamic region in prodromal Huntington disease revealed by MRI analysis. *Neurobiology of disease, 40*(3), 531-543. doi:10.1016/j.nbd.2010.07.013

Soylu-Kucharz, R., Adlesic, N., Baldo, B., Kirik, D., & Petersen, A. (2015). Hypothalamic overexpression of mutant huntingtin causes dysregulation of brown adipose tissue. *Sci Rep, 5*, 14598. doi:10.1038/srep14598

Soylu-Kucharz, R., Baldo, B., & Petersen, A. (2016). Metabolic and behavioral effects of mutant huntingtin deletion in Sim1 neurons in the BACHD mouse model of Huntington's disease. *Sci Rep, 6*, 28322. doi:10.1038/srep28322

Thompson, L. M., Aiken, C. T., Kaltenbach, L. S., Agrawal, N., Illes, K., Khoshnan, A., . . . Steffan, J. S. (2009). IKK phosphorylates Huntingtin and targets it for degradation by the proteasome and lysosome. *The Journal of cell biology, 187*(7), 1083-1099. doi:10.1083/jcb.200909067

Timper, K., & Bruning, J. C. (2017). Hypothalamic circuits regulating appetite and energy homeostasis: pathways to obesity. *Dis Model Mech, 10*(6), 679-689. doi:10.1242/dmm.026609

Trager, U., Andre, R., Lahiri, N., Magnusson-Lind, A., Weiss, A., Grueninger, S., . . . Tabrizi, S. J. (2014). HTT-lowering reverses Huntington's disease immune dysfunction caused by NFkappaB pathway dysregulation. *Brain : a journal of neurology, 137*(Pt 3), 819-833. doi:10.1093/brain/awt355

van der Burg, J. M. M., Gardiner, S. L., Ludolph, A. C., Landwehrmeyer, G. B., Roos, R. A. C., & Aziz, N. A. (2017). Body weight is a robust predictor of clinical progression in Huntington disease. *Annals of neurology, 82*(3), 479-483. doi:10.1002/ana.25007

Van Raamsdonk, J. M., Murphy, Z., Selva, D. M., Hamidizadeh, R., Pearson, J., Petersen, A., . . . Leavitt, B. R. (2007). Testicular degeneration in Huntington disease. *Neurobiology of disease, 26*(3), 512-520. doi:10.1016/j.nbd.2007.01.006

West, M. J., Slomianka, L., & Gundersen, H. J. (1991). Unbiased stereological estimation of the total number of neurons in thesubdivisions of the rat hippocampus using the optical fractionator. *The Anatomical record, 231*(4), 482-497. doi:10.1002/ar.1092310411

Zhang, X., Zhang, G., Zhang, H., Karin, M., Bai, H., & Cai, D. (2008). Hypothalamic IKKbeta/NF-kappaB and ER stress link overnutrition to energy imbalance and obesity. *Cell, 135*(1), 61-73. doi:10.1016/j.cell.2008.07.043

Zhang, Y., Reichel, J. M., Han, C., Zuniga-Hertz, J. P., & Cai, D. (2017). Astrocytic Process Plasticity and IKKbeta/NF-kappaB in Central Control of Blood Glucose, Blood Pressure, and Body Weight. *Cell metabolism, 25*(5), 1091-1102 e1094. doi:10.1016/j.cmet.2017.04.002

Zielonka, D., Marinus, J., Roos, R. A., De Michele, G., Di Donato, S., Putter, H., . . . Landwehrmeyer, G. B. (2013). The influence of gender on phenotype and disease progression in patients with Huntington's disease. *Parkinsonism Relat Disord, 19*(2), 192-197. doi:10.1016/j.parkreldis.2012.09.012

Zielonka, D., Ren, M., De Michele, G., Roos, R. A. C., Squitieri, F., Bentivoglio, A. R., . . . Landwehrmeyer, G. B. (2018). The contribution of gender differences in motor, behavioral and cognitive features to functional capacity, independence and quality of life in patients with Huntington's disease. *Parkinsonism Relat Disord, 49*, 42-47. doi:10.1016/j.parkreldis.2018.01.006

639
640 Zielonka, D., & Stawinska-Witoszynska, B. (2020). Gender Differences in Non-sex Linked
641 Disorders: Insights From Huntington's Disease. *Front Neurol, 11*, 571.
642 doi:10.3389/fneur.2020.00571
643

644

Figure 1

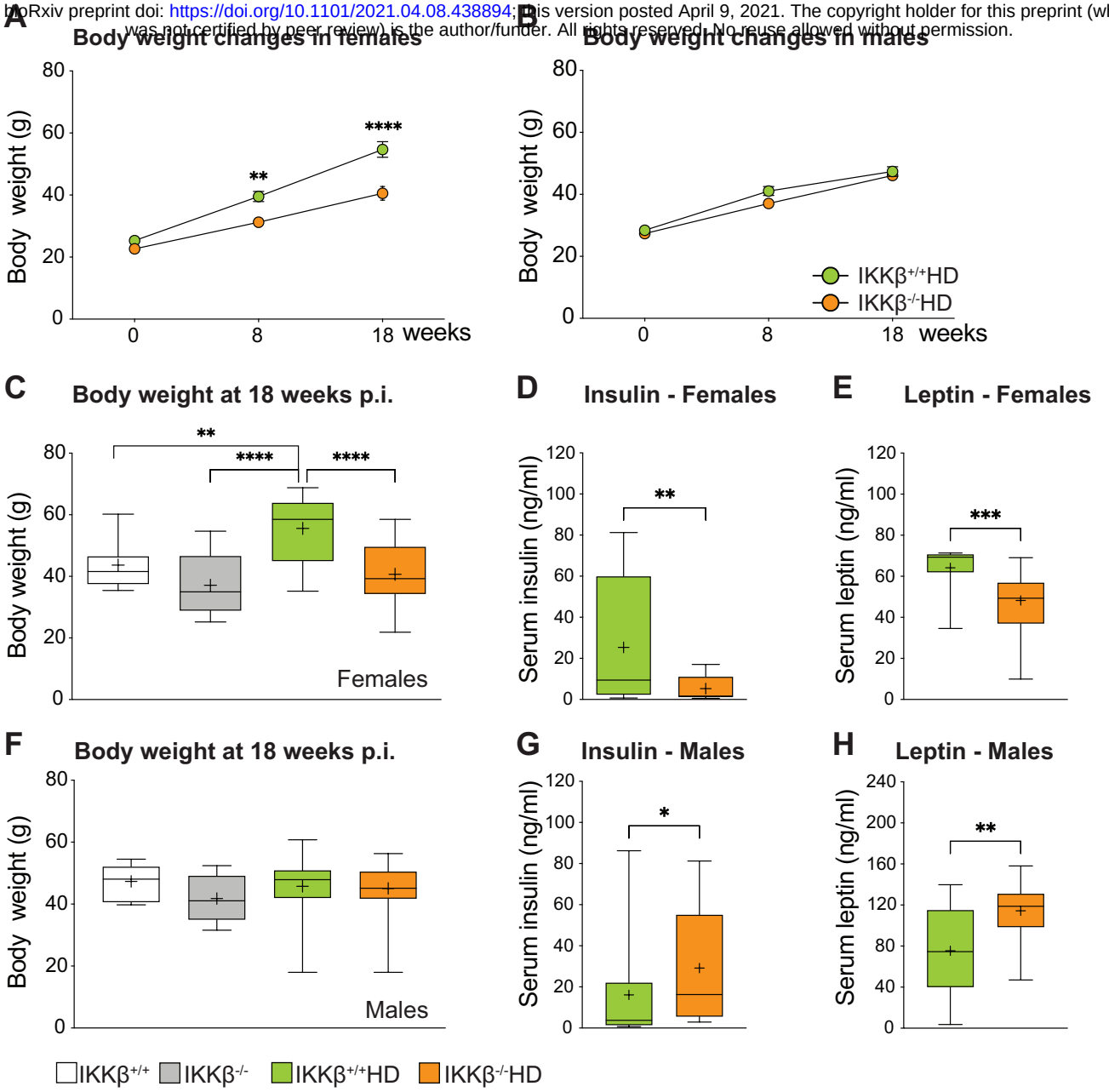

Figure 2

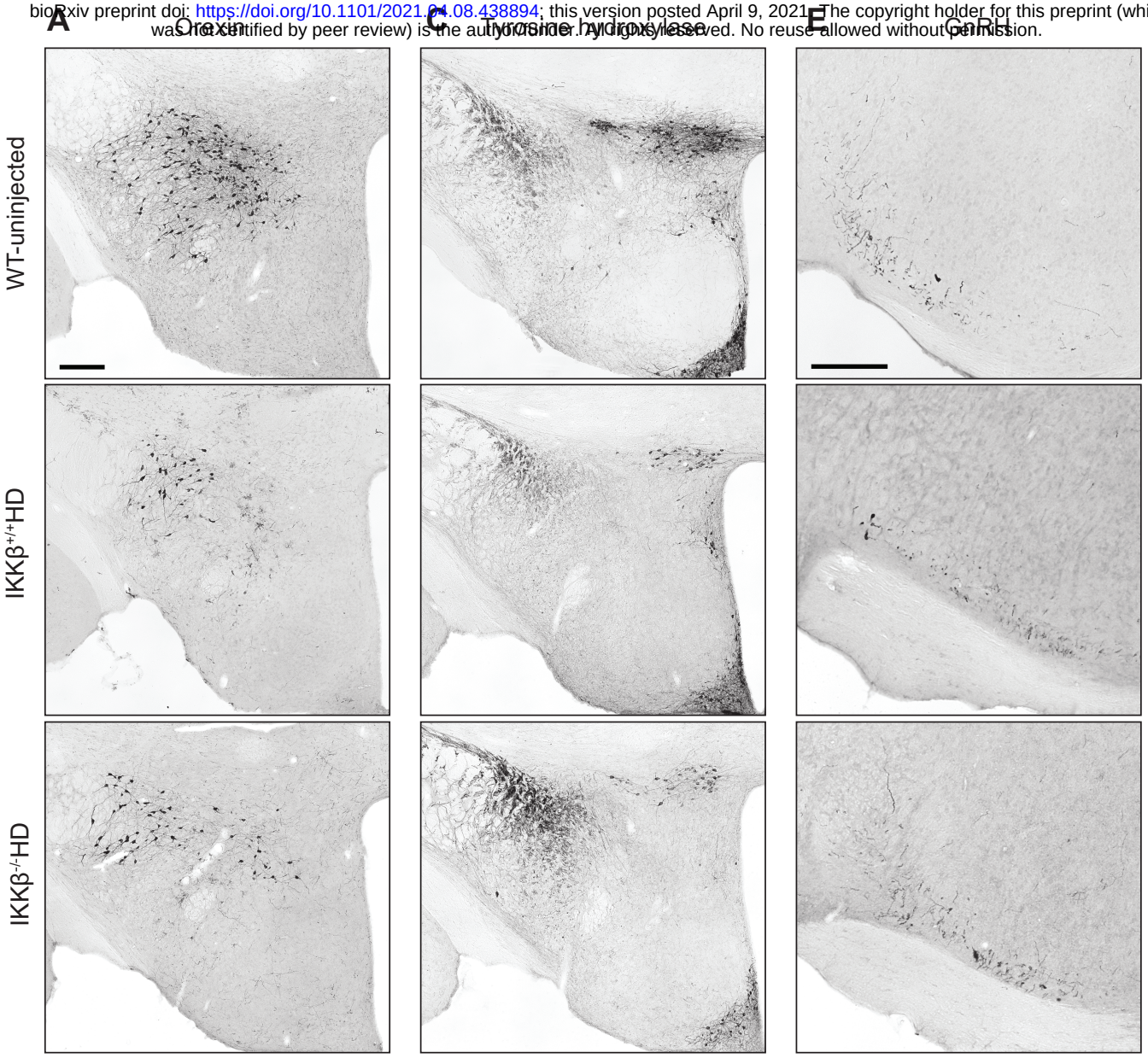

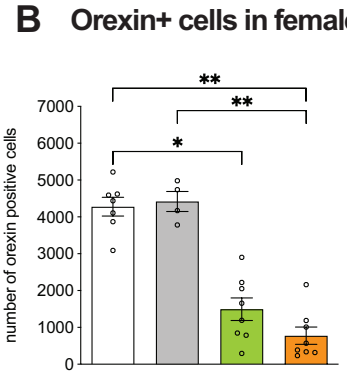

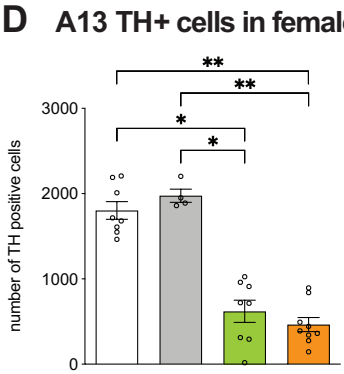

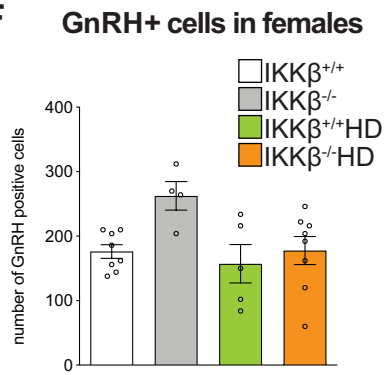

Figure 3

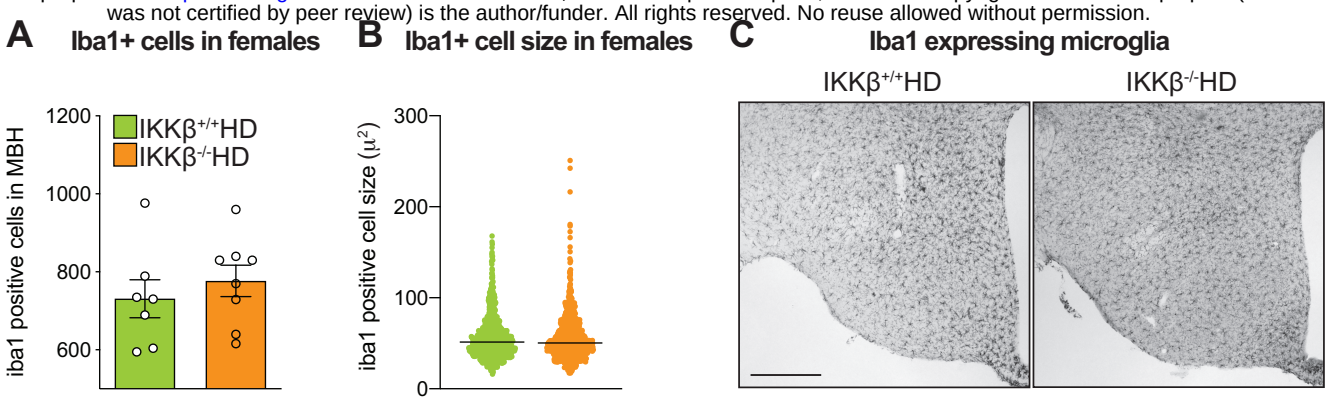

Figure 4

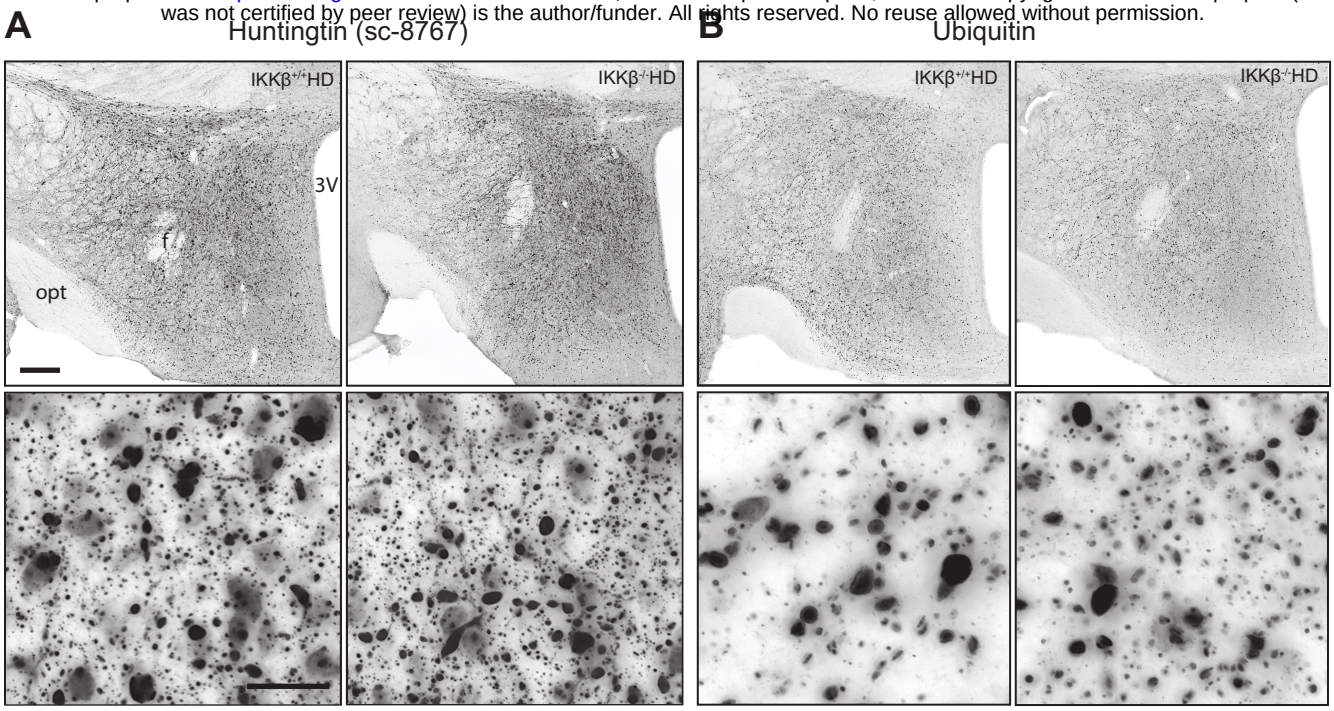

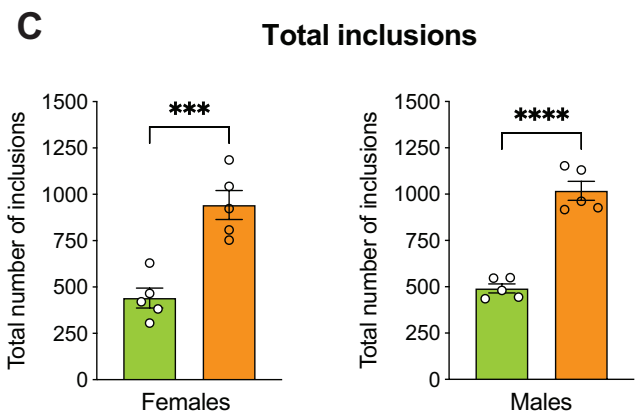

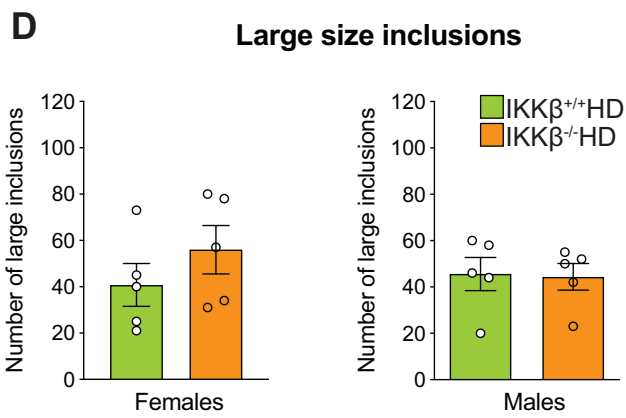

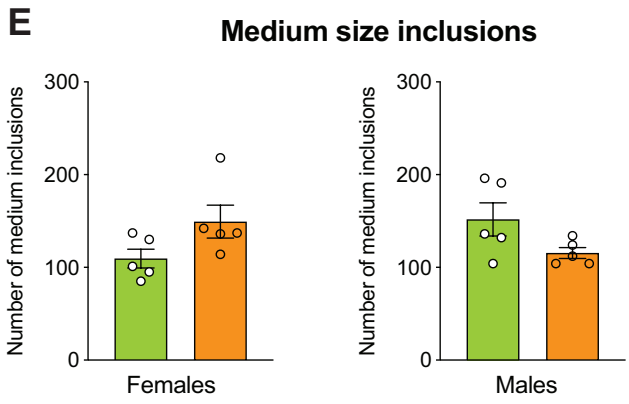

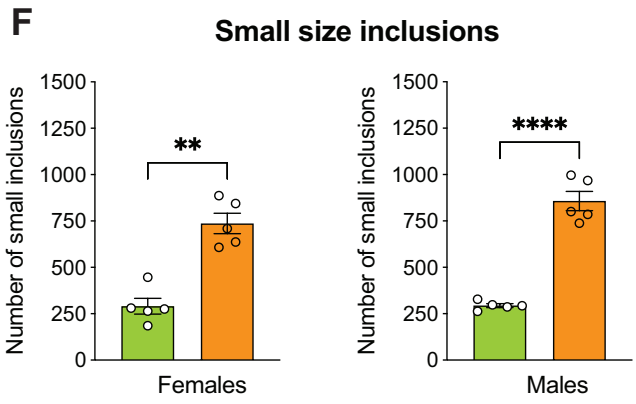

Supplementary figure 1